

See discussions, stats, and author profiles for this publication at: <https://www.researchgate.net/publication/19668423>

Optical depolarization changes in single, skinned muscle fibers. Evidence for cross-bridge involvement

ARTICLE *in* BIOPHYSICAL JOURNAL · AUGUST 1986

Impact Factor: 3.97 · DOI: 10.1016/S0006-3495(86)83439-7 · Source: PubMed

CITATIONS

8

READS

12

5 AUTHORS, INCLUDING:



Yin Yeh

University of California, Davis

111 PUBLICATIONS 2,685 CITATIONS

SEE PROFILE

OPTICAL DEPOLARIZATION CHANGES IN SINGLE, SKINNED MUSCLE FIBERS

Evidence for Cross-Bridge Involvement

R. J. BASKIN, Y. YEH,* K. BURTON, J. S. CHEN,* AND M. JONES

*Departments of Zoology and *Applied Science, University of California, Davis, California 95616*

ABSTRACT Optical ellipsometry studies of single, skinned muscle fibers conducted on the diffraction orders have yielded spectra that are sensitive to the state of the fiber. The linearly polarized light field vector becomes elliptically polarized as it passes through the fiber and may be collected at the diffraction orders. Fibers that have been subjected to extraction of myosin (0.6 M KCl) retain a weak diffraction pattern and exhibit a substantially decreased depolarization of incident linearly polarized light. A significant decrease in polarization is seen in skinned fibers that are subject to an increase in pH from 7.0 to 8.0. This increase in pH results in a decrease of ~30% in the depolarization angle of single fibers. The major decrease in depolarization angle that we observe at pH 8.0 is consistent with the notion that as cross-bridges move out from the shaft of the thick filament, their ability to cause depolarization of the incident linearly polarized light decreases (5). This interpretation is also consistent with the work of Ueno and Harrington (20) where the decrease in the ability to cross-link S-1 and S-2 to the thick filament at pH 8.2 suggests cross-bridge movement away from the thick filament. A large decrease in birefringence, seen after treatment of skinned fibers with α -chymotrypsin, appears to be related to the breakdown of myosin into rod, S-1, heavy meromyosin, and light meromyosin.

INTRODUCTION

Changes in optical depolarization (phase angle) (3) and birefringence of single skinned muscle fibers (4) during a relaxation to rigor transition have been measured. Yeh and Pinsky (3) measured the change in elliptical polarization of light diffracted from an isolated striated muscle fiber. They showed a change in the phase angle of the elliptically polarized light as the sarcomere length of the fiber was changed. Yeh et al. (5) measured depolarization changes in skinned fibers subjected to a change from a relaxed state to a rigor state. A marked decrease in phase angle was observed as the fiber passed into rigor.

In the normal transmission birefringence experiment, the measured phase shift comes from having scanned, in the forward direction, all single scattering events by the molecular elements within the path of the light beam along two mutually perpendicular polarization directions (6). Since these same molecular elements also scatter light into other directions, when we collect only light which is coherently scattered into the well-defined diffraction angle, the phase shift information is equivalent to that obtained in forward birefringence studies. Here, the phase angle δ (in degrees) is related to the birefringence, Δn , by $\delta = 360d \Delta n/\lambda$, where d is the measured path length through the fiber and λ_0 is the wavelength of the laser in

vacuum. Taylor (4, 7) measured birefringence changes accompanying relaxation of skinned, rigor fibers and reported an accompanying increase in birefringence.

One explanation for these changes, advanced by both groups of workers, is that they represent the results of cross-bridge movement and reorientation. While this hypothesis is quite attractive, experiments to date cannot be said to have established it conclusively.

Studies of birefringence (optical retardation) have been done in intact single fibers during an isometric tetanus (8). The birefringence changes were interpreted in terms of reorientation of myosin (S-1) heads. The photo-elastic modulator (PEM) ellipsometer has the advantage, however, of allowing rapid and continuous monitoring of the changes in the phase angle. The present system has a response time of 20 μ s/period. Thus myosin extraction and cleaving experiments can be monitored in situ with this system.

Evidence for pH change inducing alterations in cross-bridge orientation is provided by a number of studies. Depolarization measurements of Mendelson and Cheung (9) showed an increase in rotational mobility of the heads of synthetic filaments upon raising the pH from 6.8 to 8.3. Thomas et al. (2) have reported similar changes in the mobility of myosin heads with increasing pH, based on electron paramagnetic resonance (EPR) measurements. Chiao and Harrington (10), through measurement of the rate of cross-linking, showed that the actin-attached S-1

Dr. Chen is a Visiting Scholar from the People's Republic of China.

subunit moves out from the thick filament surface at alkaline pH. Ueno and Harrington (11) extended these studies to show that both S-1 and S-2 subunits move away from the filament surface at pH 8.0. Similar conclusions were stated by Reisler and Liu (12) after a cross-linking study that focused on synthetic myosin rod filaments. Thus a change in cross-bridge orientation after a change to an alkaline pH appears to be well-established.

A series of studies have produced evidence for myosin breakdown caused by digestion with α -chymotrypsin (1, 13, 14). Ueno and Harrington (11) determined the rates of chymotryptic proteolysis of the myosin hinge region in glycerinated rabbit fibers. While this and other studies using α -chymotrypsin were directed at determining conformational changes in the myosin hinge region, they clearly established the proteolytic effect of this enzyme on the structure of myosin. In particular, it was established that the rate of chymotryptic cleavage showed a sharp sigmoidal increase just over the pH range (increasing pH) where the rate of cross-linking S-2 to the thick filament surface underwent a precipitous decline. This result supports the notion that myosin is indeed split, under these conditions, into light meromyosin (LMM) and heavy meromyosin (HMM). (The LMM remaining in the thick filament rod, and the HMM free to diffuse away.) The conclusion that α -chymotrypsin treatment of a skinned fiber leads, under certain conditions, to cleavage and thus orientational changes in cross-bridges is well supported.

The major goal in the present investigation was to obtain evidence directly relating cross-bridge orientation to phase angle. Average cross-bridge constituents or orientation was varied in different ways. In each series of experiments, phase angle was measured concurrently with alteration of cross-bridge state. Alteration was done by myosin extraction, α -chymotrypsin treatment, and pH change.

METHODS

Background of Technique

When a light wave traverse a medium that is optically anisotropic, the polarization will change. The amount of change and the type of change depend upon the material traversed. Generally, a linearly polarized light beam will develop elliptical polarization; the extent and nature of this elliptically polarized light is determined by the polarizabilities along the various material axes and the relative phase relationship between these axes at this optical wavelength. When this measurement is performed on the diffraction pattern from a muscle fiber, optically anisotropic elements with the spatial regularity of the sarcomere are measured. Fig. 1 provides a schematic diagram of the apparatus used in this experiment. Linearly polarized laser light at $0.633 \mu\text{m}$ was sent through the stage containing the fiber. The polarization direction of incident light was controlled by a half-wave plate. Diffracted light from the fiber was collected at either first or second order through a collection system consisting of a PEM oscillating at the fundamental frequency of 50 kHz that follows the diffracted light and is followed by a polarizer oriented at -45° . The detector Stokes vector has an intensity component which is given by

$$I_D = \frac{1}{2} [I_M - U_M \cos(\delta_M \sin \omega_0 t) - V_M \sin(\delta_M \sin \omega_0 t)], \quad (1)$$

where the Stokes components $[I_M, Q_M, U_M, V_M]$ characterizes the optical

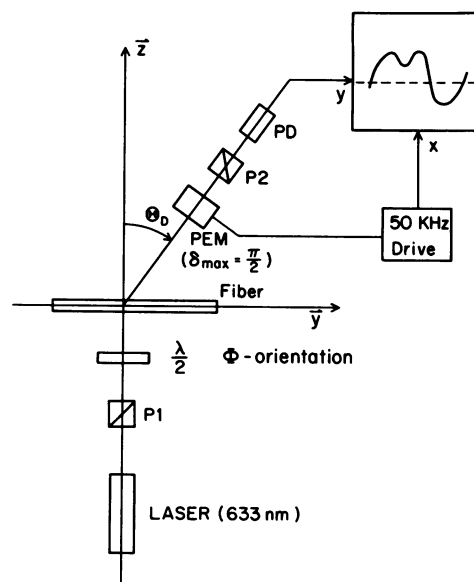


FIGURE 1 Schematic representation of experimental apparatus. P1 indicates polarizer; P2, analyzer; PEM, photo-elastic modulator; $\lambda/2$, half-wave plate; PD, polarization detector.

response of the fiber system. These four elements represent the total intensity, the intrinsic anisotropy, the 45° preference of the plane of polarized light, and the degree of circular polarization, respectively. The value of maximum shift δ_M of the PEM is preset at 90° by the calibrated magnitude of the piezoelectric driver which produces unidirectional stress birefringence on a piece of isotropic fused quartz. The intensity of the detected light may be given by

$$I_D = \frac{1}{2} [A_0 + A_1 \sin \omega_0 t + A_2 \cos 2\omega_0 t], \quad (2)$$

where the coefficients A_0, A_1, A_2 , are related to the fiber Stokes parameters by the expressions

$$\begin{aligned} A_0 &= I_M - J_0(\delta_M)U_M \\ A_1 &= -2J_1(\delta_M)V_M \\ A_2 &= -2J_2(\delta_M)U_M. \end{aligned} \quad (3)$$

From these the phase shift, δ , can be determined. Here $J_n(X)$ is the Bessel function of orders $n = (0, 1, 2, \dots)$ and argument $X = \delta_M$. $\delta = \tan^{-1} [-V_M/U_M] = \tan^{-1} [A_1 J_2(\delta_M)/A_2 J_1(\delta_M)]$. The values of A_0, A_1 , and A_2 are obtained by examining the spectral distribution directly and measuring the intensities of the spectral components at DC, ω_0 and $2\omega_0$. Even though in principle the experimentally obtainable coefficients can lead to the determination of all three muscle parameters, this method is quite sensitive to the variation of the polarization parameters and the results can easily evolve into undesirable parasitic solutions when noise is present in the data. In our tests of such an experimental system, the only truly reliable result is the value of the phase angle.

Because the dominant anisotropic element within the sarcomere is within the A-band, we discuss the changes in ellipsometry measurements based on the dynamics of an anisotropic cross-bridge element. In such an element, upon excitation, electron movement perpendicular to the helical axis was significantly faster than along the helical axis. Accordingly, light traveling the diameter of such an anisotropic region (Fig. 2A) experiences a relative optical pathlength difference. A linearly polarized light beam becomes elliptically polarized; the degree of ellipticity is dependent upon polarizabilities α_1 and α_{\perp} , and upon δ , the phase shift between these axes. If one imagines that the rod is now tilted so that the axis of the rod is along the propagation direction of the light beam, linearly polarized light

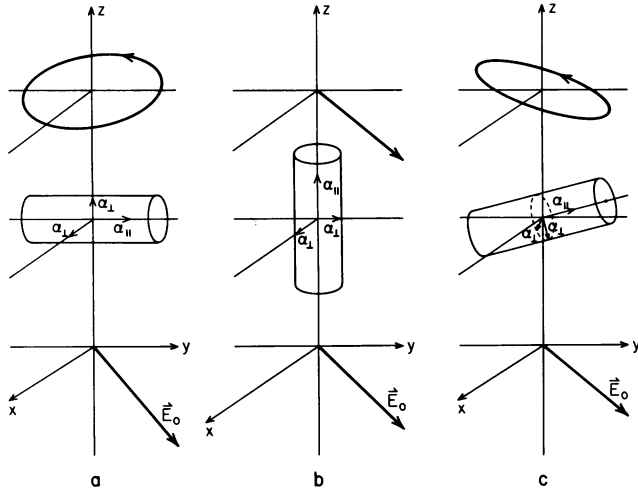


FIGURE 2 Representations of how an anisotropic element ($\alpha_1, \alpha_2, \alpha_3$) converts incident along Z-axis linearly polarized light to elliptically polarized light. (A) Element lying in the horizontal planes. (B) Element in vertical plane. (C) Element at tilt angle.

no longer experiences optical anisotropy and will remain linearly polarized (Fig. 2 B). In general, we would expect a change in δ upon simple tilt of this anisotropic rod (Fig. 2 C). If the rod is assumed not to denature, the magnitude of the polarizabilities remains fixed, thus both α_1 and α_2 would remain constant.

Calculation of Form Birefringence

The total birefringence measured in a single fiber is composed of two components. One component, intrinsic birefringence, is due to the basic atomic and molecular composition of the fiber. The second component, form birefringence, results from the macromolecular structure of fiber elements (i.e., alignment of filaments).

Form birefringence can be estimated from Wiener's Equation (15) which considers the refractive index of the filament (n_F), the medium (n_M), as well as the volume fraction of rod filaments (f). The expression is given by

$$n_e^2 - n_o^2 = \frac{f(1-f)(n_F^2 - n_M^2)}{(1+f)n_M^2 + (1-f)n_F^2} \quad (4)$$

To a first approximation this equation reduces to

$$\Delta n_F = n_e - n_o = \frac{f(1-f)(n_F^2 - n_M^2)}{2[f n_F + (1+f)n_M][(1+f)n_M^2 + (1-f)n_F^2]} \quad (5)$$

Values of f , n_F , and n_M have been measured by a number of researchers (7, 16).

Although Wiener's analysis was the first to examine form birefringence in detail, the work of Bragg and Pippard (17) provides an illuminating analysis of the same problem. If one uses the same notation as above, the form birefringence from an assembly of long, aligned rods or filaments is given by

$$\Delta n_F = \frac{n_M^2}{n_F + n_M} \left[1 + \frac{2n_F^2}{n_M^2} f - \left(\frac{n_+^2 + fn_+^2}{n_+^2 - fn_-^2} \right) \right], \quad (6)$$

where $n_{\pm}^2 = (n_F^2 \pm n_M^2)/2$. Assuming a realistic solvent index of $n_M \sim 1.40$ and a protein index $n_F \sim 1.57$, if we further assume the volume fraction to be $\sim 5\%$, then $\Delta n_F \sim 9 \times 10^{-4}$. This value is probably a high

value because hydrated proteins tend to exhibit a somewhat lower effective protein index of refraction (17). Even so, our calculated Δn_F is ~ 50 to $>60\%$ of the total measured birefringence Δn_T (Table II).

Effect of Fiber Tilt on Phase Angle

Tilt of the fiber relative to the incident beam can result in an altered value of phase angle (see Appendix). The magnitude of the alteration will depend upon the amount of the tilt as well as its direction relative to the order line being sampled. In the worst case, however, a 5° tilt will result in approximately a 2° alteration in phase angle (for $60 \mu\text{m}$ thick fiber). This error can be avoided by choosing the order line that does not show an effect of fiber tilt (until the tilt angle exceeds 20°). The way that fiber tilt effects the measurement of both form and intrinsic components of the depolarization is discussed in the Appendix.

Experimental Procedure

The lateral head of the anterior tibialis muscle from *Rana pipiens* was used in all these experiments. Skinned, single fibers are placed on a micromanipulator-controlled, cooled ($\sim 4^\circ\text{C}$) stage where light was incident through the bottom (Fig. 1). The samples were first bathed in 4 mM ATP relaxing solution. The sarcomere length (SL) of the fiber was then fixed by measuring the position of the first-order diffraction maximum. The general quality of the fiber was checked with a stereo microscope with a $40\times$ objective. The illuminated section was chosen for its uniformity in fiber diameter, absence of foreign particle adherents, and absence of visible damage. Several washes of the fiber at each ATP concentration were used to assure complete changes of ATP concentration and repeatability of the effect of washes. Measurements of the diffraction intensity and phase shift were taken at successively lower ATP concentration: 4, 2, 1, 0.5, and 0 mM. At this last stage, the fiber was in rigor. A control measurement of ellipticity at the relaxed condition constituted the completion of a single experiment.

Solution Compositions

Ringer's solution was made up of 115 mM NaCl, 2.5 mM KCl, 2.15 mM Na_2HPO_4 , 0.85 mM NaH_2PO_4 , and 1.8 mM CaCl_2 ; adjusted to pH 7.0. Three other types of solution were used in this investigation (solutions 1, 2, and 3). The ionic strength of each of these solutions was calculated by the method of Fabiato and Fabiato (18). Solution 1 has a normal ionic strength (116–134 mM) and contains 2 mM EGTA. Solution 2 has a high ionic strength (193–216 mM) and contains 30 mM EGTA. Solution 3 has a normal ionic strength but contains 30 mM EGTA. The composition of each of these solutions is listed in Table I.

Skinning Procedures

A single fiber, after having been dissected in Ringer's solution, was soaked for 30 min in relaxing solution before being skinned. The 30-min soak results in a transient contracture and is required to avoid activation of the fiber when placed in the skinning solution, presumably by removing Na^+ ions near the sarcolemma.

Four similar skinning procedures were employed during the course of this work. In procedure 1, the relaxing solution was solution 1. A fiber was placed in the skinning solution for 15 min after the 30-min soak in relaxing solution. After being skinned, the fiber was returned to relaxing solution. This procedure left the fiber ends attached to the tendons and thus in good condition and amenable to experimental analysis.

As discussed in Yeh et al. (skinning in Triton X-100 is sufficient to permeabilize the sarcolemma but not to disrupt the sarcoplasmic reticulum (SR) so as to release its store of Ca^{+2}). This conclusion results from the observation that the fiber contracts in the presence of 10 mM caffeine. We found that fibers occasionally activated if mechanically stressed, presumably due to Ca^{+2} release from an intact, though leaky, SR. To avoid such undesirable activation, skinning procedures 2–4 were employed.

TABLE 1
SOLUTION COMPOSITIONS

Solution	Relaxing solution	Rigor solution
1	96 mM KCl 9.6 mM imidazole (+ 5.8 mM HCl) 1.9 mM EGTA (+ 3.4 mM KOH) 0.96 mM MgCl ₂ 4.0 mM Na ₂ ATP (+ 7.2 mM KOH) 1.9 mM HCl added for pH 7.0 Ionic strength: 134 mM	100 mM KCl 10 mM imidazole (+ 6 mM HCl) 2 mM EGTA (+ 3.6 mM KOH) 1 mM MgCl ₂ 2 mM HCl for pH 7.0 Ionic strength: 116 mM
2	96 mM KCl 9.6 mM imidazole (+ 5.8 mM HCl) 28.8 mM EGTA (+ 5.1 mM KOH) 0.96 mM MgCl ₂ 4 mM Na ₂ ATP (+ 7.2 mM KOH) 1.9 mM HCl added for pH 7.0 Ionic strength: 216 mM	100 mM KCl 10 mM imidazole (+ 6 mM HCl) 30 mM EGTA (+ 53.6 mM KOH) 1 mM MgCl ₂ 2 mM HCl for pH 7.0 Ionic strength: 193 mM
3	24.661 mM KCl 9.6 mM imidazole (+ 5.8 mM HCl) 28.8 mM EGTA (+ 5.1 mM KOH) 1.3 mM MgCl ₂ 4 mM Na ₂ ATP (+ 7.2 mM KOH) 1.92 mM HCl for pH 7.0 Ionic strength: 140 mM	25.7 mM KCl 10 mM Imidazole (+ 6 mM HCl) 30 mM EGTA (+ 53.6 mM KOH) 1.3 mM MgCl ₂ 2 mM HCl for pH 7.0 Ionic strength: 115 mM

Unlike procedure 1, in procedure 2 the fiber was skinned for 5 min. This approach seemed to decrease the incidence of activation, perhaps due to a less permeable SR. Longer skinning times, which might have significantly removed the SR, resulted in detachment of the fiber from the tendon.

In procedure 3, the fiber was skinned for 5 min while in rigor skinning (solution 2 + 0.25% Triton). After a 5-min rinse in rigor solution (solution 2), the fiber was bathed in a rigor solution with 10 mM caffeine in order to dump the Ca²⁺ from the SR. This step was followed by a 1-h soak in rigor solution, which removed the liberated calcium. The fiber was then placed in relaxing solution. Although experimental solutions with a low concentration of EGTA (2 mM) would generally result in little activation in relaxing solution, it was found that using solution 2 (30 mM EGTA) further inhibited activation.

Procedure 4 was the same as procedure 1, except solution 2 is used. It was found that as long as a high concentration of EGTA was used in the experimental solutions after this procedure, activation in the relaxing solution could be prevented.

The removal of the fiber from the skinning solution required care that no excess skinning solution remained. The fiber was first placed in relaxing solution with ATP. Repeated rinsing with fresh relaxation solution with ATP for a few minutes was necessary to rid the fiber of residual Triton X-100.

Solution Change Procedure

Aluminum foil clips were used to support the tendon region on either end of the fiber. The clips were mounted onto pins of the micromanipulator. The chamber that contained the fiber was bathed with relaxing solution that contained the desired concentration of ATP. Each time a solution change was desired, the chamber was flushed 10 times with the appropriate solution, and experiments commenced only after a waiting period of 10 min. Repeatability of the optical experiments was assured by conducting experiments using solution rinses of the same ATP concentration. The entire chamber was maintained at 6°C by flowing coolant that was thermostatically controlled by a constant-temperature bath.

Gel Electrophoresis of Single Muscle Fibers

Each fiber was solubilized in 15 μ l of 2.5% sodium dodecyl sulfate (SDS) for 1–2 h at room temperature. The SDS-resistant cytoskeletal elements were removed and each sample mixed with 5 μ l of a sample buffer (final concentration: 0.1 M DTT; 2.4% SDS; 0.08 M Tris, pH 6.8; 10% glycerol and 0.001% bromphenol blue) and heated to 100°C for 5 min. The samples were electrophoresed on a 5–15% gradient gel with a 5% stacker gel and Tris-glycine buffer at 25 mA for ~2–3 h. Molecular weight standards at a 1:100 dilution (Bio-Rad Laboratories, Richmond, CA) were used and the gels were stained with Silver Stain (Bio-Rad Laboratories).

RESULTS

Phase Shift Accompanying Myosin Extraction

The first step in our determination of the molecular origin of the phase changes observed in single-skinned fibers was to characterize the changes accompanying myosin extraction. Fibers held at lengths between 2.6 and 3.7 μ m had their initial depolarization angle determined. After this determination they were immersed in an extracting solution containing 0.6 M KCl, and the change in depolarization angle was measured as a function of time (Fig. 3). The change in depolarization angle occurred in two distinct phases. The first phase consisted of a large, rapid decrease in depolarization and was followed by a second, slower change.

Accompanying the large decrease in depolarization angle was a 98% decrease in intensity of the order line.

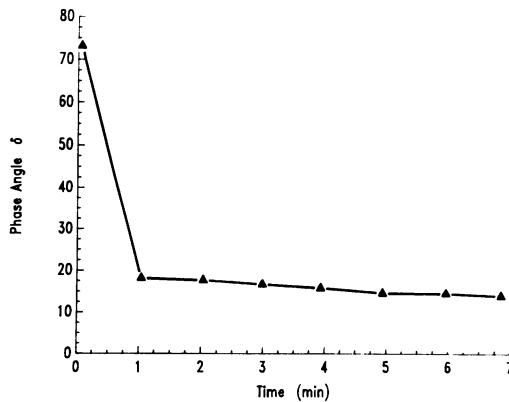


FIGURE 3 Depolarization accompanying myosin extraction. Fiber was placed in solution containing 0.6 M KCl.

Thus the majority of the structural components responsible for the light diffraction pattern were also removed. However, weak diffraction lines remained, and sampling of the phase relationships at the diffraction orders was possible throughout the experiment.

After extraction, both the fiber and the surrounding solution were analyzed on a polyacrylamide gel electrophoresis (PAGE) system that was sensitive to the extremely small protein concentrations (10 ng) present in a single fiber. The gel pattern of an intact single fiber showed numerous bands including very prominent myosin (200 kD) and actin (43 kD) bands. Following extraction with 0.6 M KCl the myosin band virtually disappeared, and was found in the bathing solution (Fig. 4).

Thus both the PAGE data and the intensity decrease in the diffraction orders support the notion that myosin extraction has occurred parallel with the large decrease in depolarization angle.

Reproducibility of the Relax-Rigor Transition

Fig. 5 shows four relax-rigor transitions on the same fiber. In each case the relaxed fiber was put into rigor by passing through two successive ATP concentrations (1 and 0.5 mM). The variability between runs depended somewhat on ATP concentration, but the average SD was $\pm 1.0^\circ$. (In each run the rigor fiber was placed directly in the relaxing solution [4 mM ATP] in preparation for the next run.)

Change in Fiber Diameter with Change in pH

Several authors have reported a change in lattice spacing accompanying pH change (see Discussion). While there appears to be no agreement as to the magnitude of the change, all of the reports show a direct relationship between pH and lattice volume (i.e., $\Delta pH \sim \Delta V_{\text{lattice}}$). Since depolarization angle is dependent upon fiber thickness (diameter) we examined a series of fibers optically and

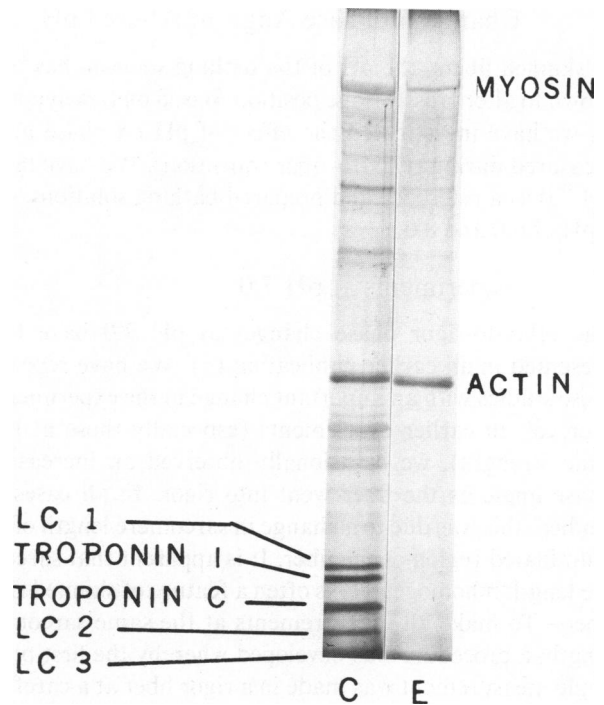


FIGURE 4 SDS-PAGE of fiber after extraction in 0.6 M KCl for 30 min. Lane C shows pattern from control fiber and lane E shows pattern from extracted fiber. Note large decrease in 200-kD bands as well as light chain bands. (Band identification was on the basis of approximate molecular mass.)

determined fiber diameter changes as we changed pH. As pH was lowered to 6.0 from 7.0 we measured an average decrease (10 experiments) of 4.1% in fiber diameter. When the pH was raised from 7.0 to 8.0 we measured an average increase (8 experiments) of 2.6%. It can be shown using the Wiener Equation for form birefringence that a 4.1% decrease in fiber diameter would result in an approximate depolarization increase of 8.2%. Similarly, a 2.6% diameter increase leads to a 5.2% decrease in depolarization angle.

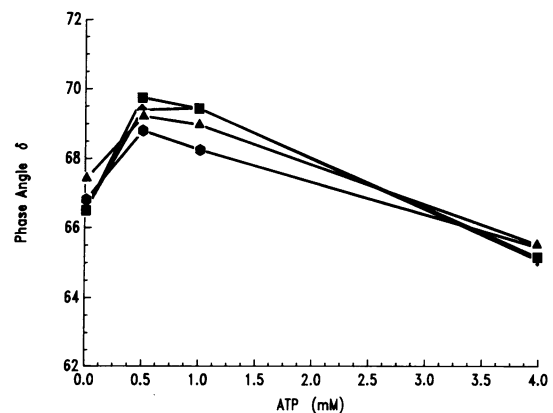


FIGURE 5 Reproducibility of the relax-rigor transition. Four relax-rigor transitions on the same fiber. SD at each ATP concentration was $\pm 1.0^\circ$ or less. (pH 7.0).

Changes in Phase Angle at Altered pH

In skinned fibers, the pH of the bathing solution has been shown to alter cross-bridge position. Based on this hypothesis we have investigated the effect of pH on phase angle measured during relax-to-rigor transitions. We have taken pH 7.0 as a reference and prepared bathing solutions with a pH of 6.0 and 8.0.

Experiments at pH 7.0

The relax-to-rigor phase changes at pH 7.0 have been presented in an earlier publication (5). We have repeated these studies with an important change in the experimental protocol. In earlier experiments (especially those at high ionic strength), we occasionally observed an increase in phase angle as the fiber went into rigor. In all cases we studied, this was due to a change in sarcomere length of the illuminated region of the fiber. It is apparent that sarcomere length inhomogeneity is often a feature of skinned rigor fibers. To make all measurements at the same sarcomere length, a procedure was developed whereby the first phase angle measurement was made in a rigor fiber at a carefully determined sarcomere length. The second measurement was made after relaxation of the fiber and a resetting of the sarcomere length to the rigor value.

The birefringence change accompanying the rigor-to-relax transition at a series of sarcomere lengths is presented in Table II. In all cases the rigor birefringence is

less than the relaxed value and the transition results in an increase in Δn . The range of the change in Δn was from 0.2×10^{-3} to 0.27×10^{-3} and showed the same relationship to sarcomere length as previously reported (5). In four cases (fibers 2-5, 3-6 [reference 13]; 3-7, 2-21; 2-27, 2-15 [reference 19]; and 2-20 [reference 13], 3-26), fibers at or near the same sarcomere length showed a large difference in $d\Delta n$. The average value of $d\Delta n$ was $0.12 \pm 0.08 \times 10^{-3}$ when calculated from the 0.5 mM ATP relaxed value and $0.11 \pm 0.10 \times 10^{-3}$ when calculated from the 4.0 mM ATP relaxed value. However, in any given fiber $d\Delta n^*$ was almost always larger than $d\Delta n^\ddagger$, reflecting the slight difference in δ usually seen between 4 mM ATP and 0.5 mM ATP. As will be discussed later, the variability in the change in Δn may result from a real difference in average cross-bridge position in rigor fibers (i.e., the rigor state may not be precisely defined; average cross-bridge position may vary from one rigor state to another).

Variation in Phase Angle with Position Along a Given Fiber

Some variation is seen in phase angle (pH 7.0) at different positions along a single fiber even when care is taken to measure locations only with the same sarcomere length. The two positions in Fig. 6 were an "end" and a "center" region. Since fibers are generally oval in cross-section, a slight twist in the fiber will result in a different path length

TABLE II
BIREFRINGENCE CHANGE ACCOMPANYING RELAX-TO-RIGOR TRANSITION
AT CONSTANT SARCOMERE LENGTH (pH = 7.0)

Fiber	Sarcomere length	Δn Rigor	Δn Relax (0.5 mM ATP)	Δn Relax (4 mM ATP)	$d\Delta n^*$	$d\Delta n^\ddagger$
	μm	$\times 10^{-3}$	$\times 10^{-3}$	$\times 10^{-3}$	$\times 10^{-3}$	$\times 10^{-3}$
2-15(1)	2.11	1.83	1.87	2.86	0.04	0.03
2-5	2.22	1.59	1.86	1.83	0.27§	0.24
3-6(1)	2.25	1.41	1.55	—	0.14§	—
3-6(2)	2.31	1.73	1.85	—	0.12	—
3-8	2.36	1.77	1.86	—	0.09	—
3-7	2.36	1.84	1.86	—	0.02§	—
2-21	2.37	1.71	1.91	1.76	0.20§	0.05
2-27	2.45	1.35	1.61	1.57	0.26§	0.22
2-15(2)	2.49	2.21	2.24	—	0.03§	—
2-26	2.52	1.62	1.71	1.66	0.10	0.05
3-11	2.58	1.98	2.16	—	0.18	—
2-15(3)	2.63	2.03	2.16	2.15	0.13	0.12
2-20(1)	2.71	1.76	1.93	1.81	0.17	0.05
2-20(2)	2.86	1.65	1.88	1.89	0.23§	0.24
3-26	2.89	1.54	1.60	—	0.06§	—
2-19	3.04	1.66	1.70	1.67	0.04	0.01
2-20(3)	3.10	1.77	1.80	—	0.03	—
3-20	3.10	2.03	2.08	—	0.05	—
($n = 18$)		1.75 ± 0.22	1.87 ± 0.20		0.12 ± 0.08	
($n = 9$)				1.79 ± 0.17		0.11 ± 0.10

*Birefringence difference between rigor and 0.5 mM ATP relaxed state.

‡Birefringence difference between rigor and 4.0 mM ATP relaxed state.

§Fibers with second fiber at or near the same sarcomere length but large difference in $d\Delta n$.

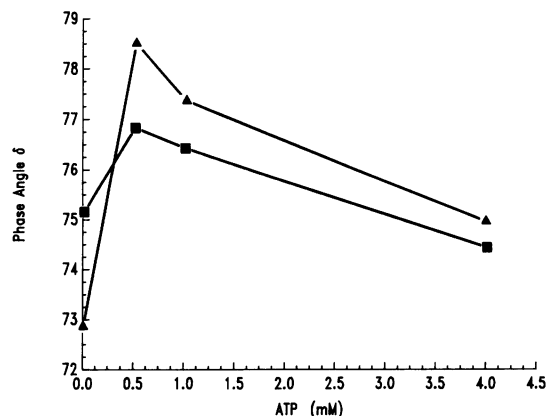


FIGURE 6 Variation in phase angle with position along a fiber. ■, center for fiber; ▲, end region of fiber.

of the beam through the fiber. An analysis of our data (at $SL = 2.4 \mu\text{m}$) shows a value of δ of $\sim 0.9^\circ/\mu\text{m}$ of muscle. Thus a $10\text{-}\mu\text{m}$ difference in path length would generate a 9° difference in δ . The differences in δ , seen in Fig. 6, are small and could easily result from a difference in path lengths through the fiber.

Experiments at pH 6.0

To evaluate δ at pH 6.0, the following experiment was done. The value of δ for a fiber at a given ATP concentration and a pH 7.0 was determined. The pH of the solution (at the same ATP concentration) was lowered to 6.0 and δ measured. The fiber was then returned to a pH of 7.0 before repeating this process at a different ATP concentration. The results are shown in Fig. 7. As pH is lowered (to 6.0), the value of δ increases, although the increase is small. This experiment was repeated using 15 fibers and a total of 22 changes in pH at the four different ATP concentrations. In 77% of the runs the value of δ increased upon decreasing the pH to 6.0. The average percent increase in birefringence accompanying this change was 5.53 ± 4.28 . This may be explained as the result of changes in fiber diameter caused by the lower pH (see Discussion).

Experiments at pH 8.0

Experiments in which the pH is raised to 8.0 were carried out. Raising a fiber to this pH resulted, in some cases, in fiber activation. Waves of contractions passed along the length of the skinned fibers. This problem was largely eliminated in the high ionic strength solutions however, by raising the EGTA concentration from 2 to 30 mM (solution 2 of Table I). It is likely that the observed activation resulted from the release of calcium induced by the increase in pH.

Change of pH from 7.0 to 8.0 (Fig. 7) results in a decrease in δ . In all, 17 fibers were studied. Normally, pH was increased while the fiber was in a relaxed (1–4 mM ATP) state. In 20 transitions, from either pH 7.0 to pH 8.0 or pH 8.0 to pH 7.0, the phase angle δ was always lower at

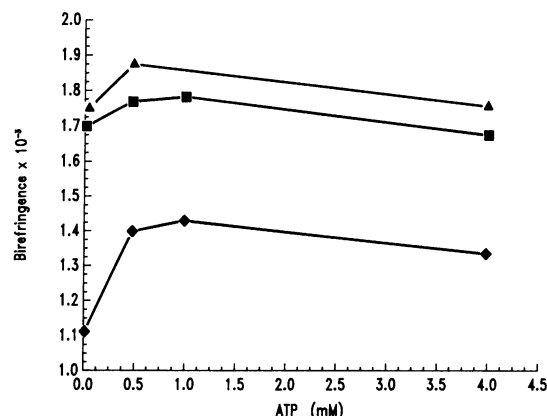


FIGURE 7 Birefringence as a function of ATP, concentration at three different values of pH. ■, pH 7.0; ▲, pH 6.0; ♦, pH 8.0.

pH 8.0. In six relaxed (4 mM ATP) fibers, a decrease in birefringence of $16.75 \pm 8.6\%$ accompanied a change in pH from 7.0 to 8.0. This decrease was larger than could be accounted for by change in fiber diameter following the pH change.

pH Change in Rigor Fibers

Skinned fibers were placed into rigor at pH 7.0. We then changed the fiber pH either to 6.0 or 8.0. This experiment was done on 20 fibers. In all, 22 changes of pH were made and in only three changes was a marginally significant change ($\pm 2.5^\circ$) in phase angle (δ) observed. The very strong conclusion is that rigor fibers, with cross-bridges locked onto thin filaments, show little change in phase angle upon change in pH. Since our hypothesis requires that cross-bridge movement accompany pH change (in relaxed fibers), we may infer that rigor fiber cross-bridges cannot move upon alteration in the fiber pH. This provides support for the notion that cross-bridge positional changes determine the changes measured in the phase angle (δ).

α -Chymotrypsin Studies

The proteolytic enzyme α -chymotrypsin has been used to detect structural changes in the S-2 region of myosin when cross-bridges were released from the thick filament surface after an increase in pH (14, 20). We have studied the phase change following α -chymotrypsin treatment of relaxed and rigor fibers at different sarcomere lengths.

The addition of α -chymotrypsin, even at a low concentration ($2 \mu\text{g/ml}$), to a skinned fiber (4°C) held at various sarcomere lengths in relaxing solution (4 mM ATP), results in a rapid decrease in phase angle (Fig. 8). The curves shown are for sarcomere lengths of 3.8 and $2.15 \mu\text{m}$. Note that the drop in δ is more rapid in the overlap condition. This may be related to the effect of α -chymotrypsin on troponin (14). Following the measurement of phase angle, the fiber was subjected to analysis by SDS-PAGE (Fig. 9). The resulting gel (5-min incubation in $5 \mu\text{g/ml}$ α -chymotrypsin) showed clear changes when

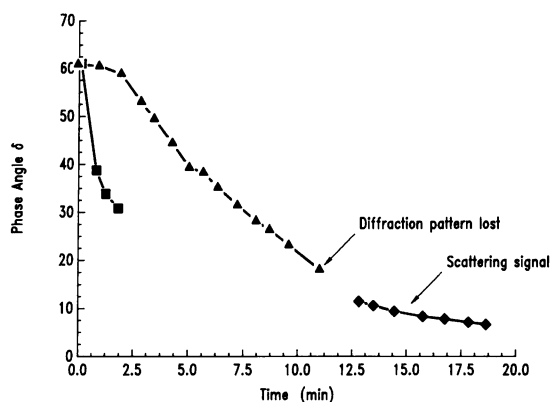


FIGURE 8 Change in phase angle after treatment with 2 $\mu\text{g/ml}$ α -chymotrypsin. \blacktriangle , sarcomere length = 3.8 μm (no overlap); \blacksquare , sarcomere length = 2.15 μm . \blacklozenge , scattering signal monitored after diffraction order disappeared.

compared with an untreated fiber. Fig. 9 *B*, lane *B* shows the protein bands observed in an untreated (control) fiber. All of the remaining lanes, except for the standards Fig. 9 *A*, lane *D*, and Fig. 9 *B*, lane *A*, show the presence of a

band at an approximate molecular mass of 125 D. This we presume to be the rod (monomer) portion of the myosin molecule. The other lanes contain relaxed (4 mM ATP) and rigor fibers at overlap (sarcomere length = 2.3 μm) and beyond overlap (sarcomere length = 3.8 μm). Fig. 9 *A*, lane *A* contains a rigor fiber (2.3 μm), as does Fig. 9 *B*, lane *D* (3.8 μm) and both of these gels show the presence of myosin S-1. On the other hand, Fig. 9 *A*, lanes *B* and *C* contain relaxed fibers and show no S-1 band, presumably because the cleaved S-1 was free to diffuse out of the fiber. No difference is seen in the gels of different sarcomere lengths when all other conditions are the same.

After treatment of the fiber (SL = 3.8 μm) with 2 $\mu\text{g/ml}$ α -chymotrypsin (4°C) for ~10–12 min, the diffraction pattern was lost. The enzymatic treatment resulted in disruption of sarcomere integrity as observed microscopically.

After the disappearance of the diffraction pattern, we monitored the scattering signal for several minutes. The very low value of depolarization (phase) angle reflects the lack of structural orientation in the enzymatically disrupted fiber.

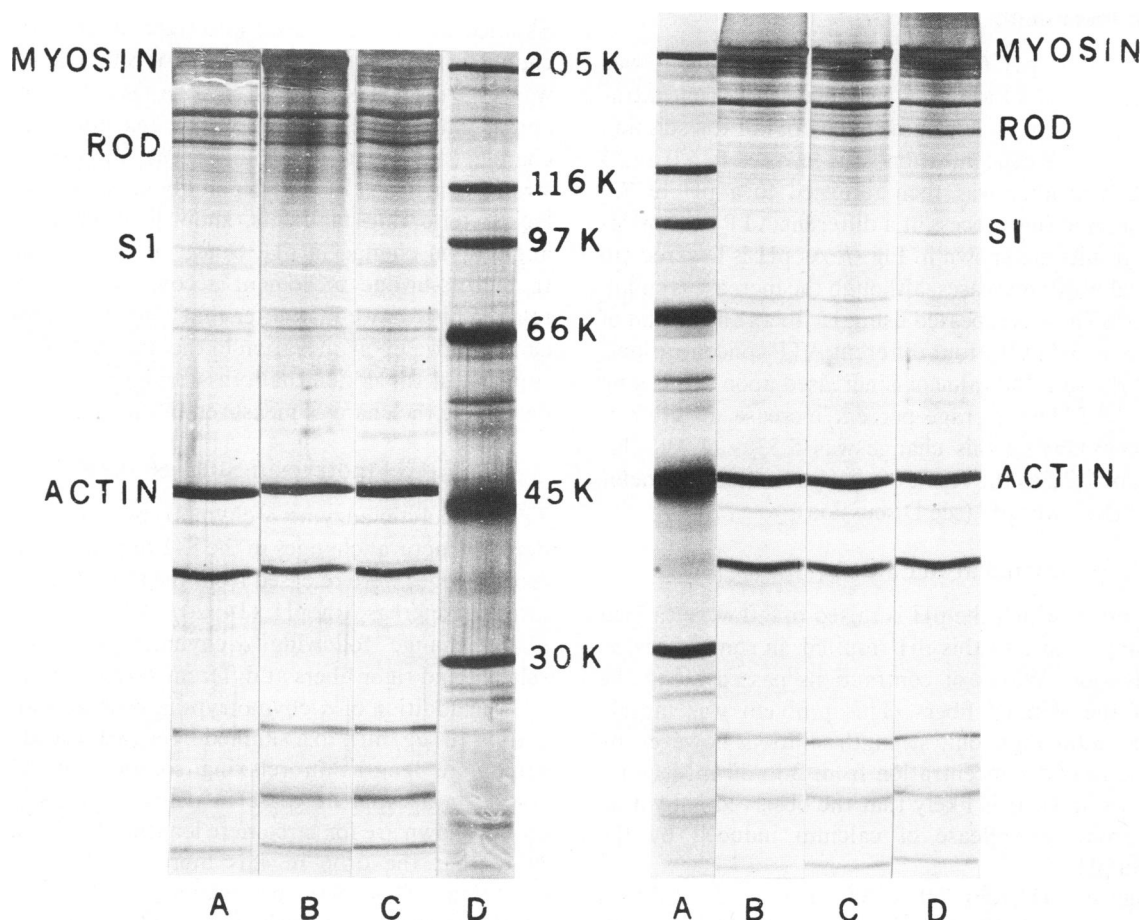


FIGURE 9 SDS-PAGE of single fibers after treatment with 5 $\mu\text{g/ml}$ α -chymotrypsin (5 min). *A*: lane *A*, rigor fiber, SL 2.3 μm ; lane *B*, relaxed fiber, SL 3.8 μm ; lane *C*, relaxed fiber, SL 2.3 μm ; lane *D*, high molecular mass standards. *B*: lane *A*, high molecular mass standards; lane *B*, control fiber, no α -chymotrypsin treatment; lane *C*, relaxed fiber, SL 3.8 μm ; lane *D*, rigor fiber, SL 3.8 μm .

Rigor Fibers

When treatment with 2 $\mu\text{g}/\text{ml}$ α -chymotrypsin (4°C) was repeated in rigor fibers, the results differed from the relaxed fiber. Little change in depolarization angle was observed (Fig. 10). Initially only a slow decrease in depolarization is seen; however, the introduction of ATP (1 mM) results in a dramatic change. Following the ATP addition, a rapid decrease in phase angle occurs. This continues until the diffraction pattern is lost at a phase angle of $\sim 18^\circ$. This ATP effect most likely has a twofold origin. First, cleavage of myosin into rod, S-1, HMM, and LMM appears to depend, in part, upon the concentration of Mg-ATP (11, 20). Second, the cleaved HMM fragment would not be free to diffuse away from the thin filament in the absence of ATP. The actin-S-1 bond will restrict the movement of the HMM fragment.

This same experiment was done on fibers with sarcomere lengths of 2.1, 2.8, and 3.8 μm . In each case a similar result was observed (data not shown). The slow initial decrease lasted until the introduction of ATP. A rapid decrease in phase angle followed by a loss of the diffraction pattern always followed ATP introduction.

SDS-PAGE of rigor fibers treated with 5 $\mu\text{g}/\text{ml}$ α -chymotrypsin for 5 min (4°C) showed significant changes from an untreated fiber (Fig. 9). When the α -chymotrypsin concentration is increased 40-fold to 200 $\mu\text{g}/\text{ml}$, two other bands are observed in the gel. A heavy band at ~ 140 kD(HMM) and a lighter band at 66 kD(LMM) (Fig. 11). Thus, cleavage of the myosin molecule clearly can occur in a skinned fiber in the absence of ATP.

The change in phase angle in rigor fibers treated with 200 $\mu\text{g}/\text{ml}$ (22°C) α -chymotrypsin was also determined (Fig. 12). A steady decrease in phase angle over a time course of several minutes was observed. Taken with the gel results (Fig. 11), we conclude that the decrease in phase angle resulted from the cleavage of myosin into HMM and LMM fragments and possibly, in some molecules, into rod

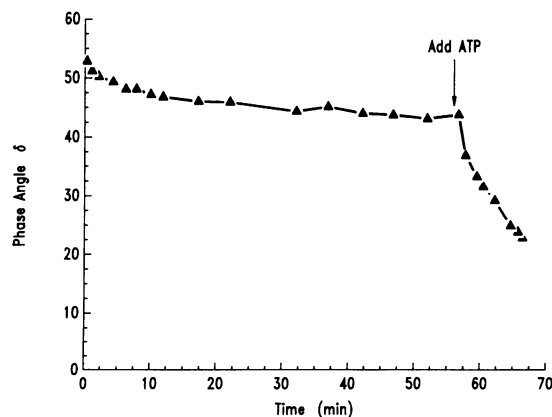


FIGURE 10 Phase angle change after treatment with α -chymotrypsin (2 $\mu\text{g}/\text{ml}$) of a rigor (0 mM ATP) fiber. The addition of ATP (arrow) causes a rapid decrease.

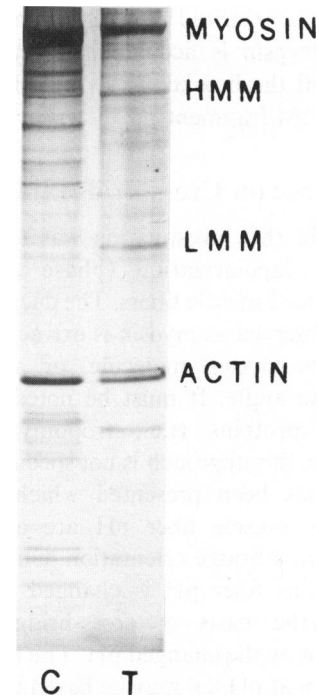


FIGURE 11 SDS-PAGE of single rigor fiber after treatment with 200 $\mu\text{g}/\text{ml}$ α -chymotrypsin for 5 min. SL = 2.8 μm ; 0 mM ATP. C, untreated fiber; T, treated fiber.

and S-1. The decrease in phase angle under these conditions (0 mM ATP) was much slower than when ATP was present. The decrease reflects the randomization of cross-bridge position due to rotational mobility of HMM while attached to thin filament actin.

DISCUSSION

This investigation has established the following: (a) Skinned single fibers show a decrease in depolarization angle as myosin is extracted. A weak diffraction pattern with little phase shift remains even after extensive removal of myosin. (b) Changes in fiber pH produce changes in phase angle that are consistent with the hypothesis that cross-bridge

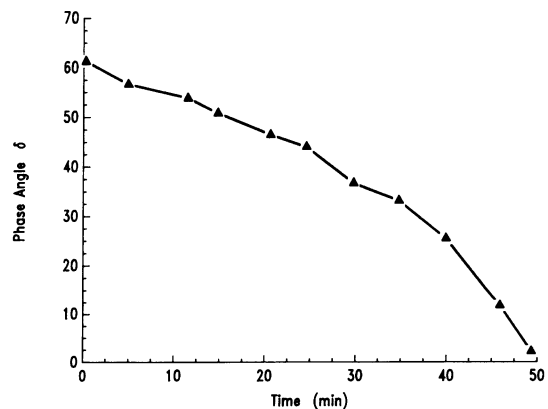


FIGURE 12 Change in phase angle in rigor fiber after the addition (at time zero) of 200 $\mu\text{g}/\text{ml}$ α -chymotrypsin. (SL = 2.6 μm .)

reorientation has occurred. (c) The treatment of fibers with α -chymotrypsin is accompanied by a decrease in phase angle and the breakdown of myosin into rod, S-1, HMM, and LMM fragments.

Evidence for Cross-Bridge Involvement

A major goal of this investigation was to determine the origin of the depolarization (phase angle) changes observed in skinned muscle fibers. The decrease in depolarization angle observed as myosin is extracted supports the notion that the myosin molecule, or a portion of it, influences phase angle. It must be noted, however, that other muscle proteins (i.e., tropomyosin) are also extracted. Thus, this approach is not specific for myosin.

Evidence has been presented which indicates that changes in the muscle fiber pH are accompanied by alterations in cross-bridge orientation. Our measurements of phase angle as fiber pH is changed are most easily explained on the basis of cross-bridge orientational changes induced by the changed pH. The large decrease in phase angle seen at pH 8.0 may be based in the movement of HMM or S-1 away from the filament backbone. The increase in phase angle at pH 6.0 suggests a more tightly packed (i.e., against the thick filament) orientation of HMM or S-1.

The enzyme α -chymotrypsin is known to split myosin as well as effect the regulatory protein troponin. We have measured changes in phase angle during incubation of fibers with α -chymotrypsin and found that under certain conditions, decrease in phase angle is correlated with the breakdown of myosin into rod, S-1, HMM, and LMM fragments. After low level enzymatic treatment (2 μ g/ml) in a rigor fiber, little change in phase angle is observed. Immediately upon the relaxation of the treated fiber, by the introduction of ATP, a large decrease in phase angle is seen. In contrast, relaxed fibers show a rapid change in phase angle upon α -chymotrypsin treatment. While it is clear from the SDS-PAGE studies that myosin is cleaved by the enzyme whether in a relaxed fiber or in a rigor fiber, it is not possible to say with certainty exactly what molecular changes are responsible for the decrease in phase angle. The interpretation is further complicated by the apparent sarcomere disorganization occurring at some time following enzyme treatment of a relaxed fiber.

Under our experimental conditions, low concentrations of enzyme (2–5 μ g/ml) and short incubation times (5–10 min) resulted in cleavage of myosin into rod and S-1 fragments. These enzyme concentrations may also have effected troponin (11) and contributed to the activation observed when ATP was present.

On the other hand, large quantities of enzyme (200 μ g/ml) for several-minute incubations showed prominent HMM and LMM fragments, as well as a decrease in phase angle.

It is interesting to note that even in the “no-overlap”

(3.8 μ m sarcomere length) rigor fiber, S-1 was trapped in the fiber, presumably on actin filaments.

Thus, myosin extraction, change in pH, and treatment with α -chymotrypsin all result in phase angle changes consistent with the hypothesis that cross-bridge position influences the phase angle (birefringence) measured in a skinned muscle fiber.

Birefringence Changes Accompanying Relax-to-Rigor Transition

The birefringence changes accompanying the relax-to-rigor transition presented in Table II show an interesting anomaly. In four cases, a large difference (>0.13) is seen at or near the same four sarcomere lengths. Since a variation of 1° in δ leads to a Δn of 0.03×10^{-3} (60 μ m diam fiber), a variation of $>4^\circ$ would be required in each case. Since our variation upon repeated measurement in the same fiber is $\sim 1^\circ$, some other factor must be involved. A major uncertainty in these studies as we are now able to conduct them is the correct value of fiber diameter in the illuminated region at the time of measurement of phase angle. Needless to say, precautions are taken to measure the same region of the fiber in both the relaxed and rigor states; however, it is not possible to say with certainty, in all cases, that this has been accomplished.

A second possibility is that there may exist different average cross-bridge configurations in rigor, that is, rigor may not represent a single configurational state of strained muscle.

Support for this notion comes from several studies. Kawai and Brandt (21), using skinned crayfish muscle fibers, found that the rigor state was not unique but depended on the condition of the fiber before rigor. They were able to characterize both a “low rigor” and a “high rigor” state. Low rigor fibers developed a small tension and moderate stiffness while high rigor fibers maintained near peak tensions and developed a high stiffness.

In a series of measurements of radial stiffness of frog fibers, Umazume and Kasuga (22) concluded that some factor, in addition to a number of attached cross-bridges, has to be considered in order to explain their results. They suggested that there may be variability in the manner of cross-bridge attachment. This suggests that different configurational states of rigor cross-bridges may exist.

Evidence for two different cross-bridge configurations in rigor muscle has been presented by Taylor et al. (23). Using a computer-based system, they obtained three-dimensional density maps that revealed a different tilt of lead and rear bridges within each double chevron. The lead bridges appeared tilted $\sim 50^\circ$ to the filament axis and the rear bridges appeared to be angled nearly normal (78°) to the filament axis.

It is possible that certain conditions favor one cross-bridge configuration over the other. Thus it may be that average cross-bridge configuration in rigor muscle does

indeed vary, and forms the basis for the variation in the difference between relax and rigor values of birefringence that we observed.

Volume Changes Accompanying pH Changes

Since depolarization angle is a function of fiber thickness, any change in thickness (or volume) accompanying the pH change would have to be accounted for. The effect of pH on lattice spacing has been reported by several authors. Rome (27) found that $d(1,0)$ varied directly with pH in the range 6.3 to 7.9, showing a 20% change at pH 6.3 (relative to pH 7.0). Her fibers were in a glycerol solution (rigor) and maintained a constant volume with varying sarcomere length. In a subsequent investigation, Rome (16) showed that an approximately linear relationship (slope $\cong 14$ Å/pH unit) exists between $d(1,0)$ and pH over a range from pH $\cong 4.0$ to pH = 9.0. This is equivalent to a change of $\sim 5\%$ in lattice spacing per 1 pH unit (fiber in salt solution). On the other hand April et al. (19), using mechanically skinned crayfish fibers in a relaxing solution, show a change in fiber volume near to 20% per unit of pH change.

In mechanically skinned frog semi-tendons fibers, Matsubara and Elliott (25) found no effect of ΔpH on lattice spacing. Millman et al. (26) reported a decrease in lattice spacing with decreasing pH of $\sim 5\%$ per pH unit.

Thus, while most authors show a decrease in lattice volume with a decrease in pH (in skinned fibers), the magnitude of the change varies from $<5\%$ to as much as 20% per pH unit. In our measurements of fiber diameter with altered pH we find a change of between 2.6 and 4.1%. This corresponds to a volume change of between 5.2 and 8.2%. Thus the change in birefringence observed upon changing pH from 7.0 to 6.0 may be due solely to the change in lattice spacing and the resulting thinner fiber. The birefringence change upon raising the pH to 8.0 is, however, much larger than can be explained by changes in fiber diameter.

Variation in Fiber Diameter

The measured value of phase angle is dependent on both the thickness and the birefringence of the fiber. Indeed, a major source of the small variation in phase angle seen at different locations along a fiber probably results from small differences in fiber diameter. Blinks (27) has shown that, while cross-sectional area is remarkably constant along most of the length of an isolated single fiber, fiber shape (and therefore thickness) is not. Since depolarization angle (and birefringence) is dependent on thickness, considerable variation from region to region is possible. Indeed, this almost certainly explains the differences in phase angle (δ) found between different regions of the same fiber. The photographs of muscle cross-section presented by Blinks (27) show a variation in thickness of

$\pm 15\%$. (In an infrequently observed "strap-like" fiber the variation in thickness would be even greater). While we did observe a variation in phase angle between different regions of the same fiber as large as 15–25%, we studied only those fibers where the variation was $<5\%$ (except in rigor).

Fiber Diameter Changes Accompanying Rigor to Relax Transition

Rome (16) reported no change in lattice spacing as rigor fibers were relaxed in specimens with sarcomere lengths from 2.0 to 3.0 μm . In a later paper (28), however, some indication of an increase in lattice spacing upon relaxation was seen at sarcomere lengths below 2.5 μm . At sarcomere lengths above 3.0 μm a decrease in $d(1,0)$ upon relaxation was observed. In our investigation, the changes we observed in the phase angle of fibers undergoing a relax-to-rigor transition were not dependent upon sarcomere length. Taylor (7) reported a 2% change in fiber diameter (SL = 2.9 μm) when rigor fibers were relaxed. It can be shown, based on the Wiener Equation, that this would result in a 4% change in form birefringence. Most of the relax-to-rigor changes presented in this investigation and in an earlier investigation (5) are larger than can be explained by these lattice spacing changes.

APPENDIX

Depolarization of Light in a Resting Fiber: Effect of Changes in Incident Angle

In discussing the effect of changing incident angle upon the depolarization of light in a resting fiber, we will first calculate the effect on the intrinsic component (δ_i) and use the simple approximation

$$\delta_{\text{total}} = \delta_{\text{form}} + \delta_i;$$

$$\text{and } 2\delta_i = \delta_{\text{form}}.$$

This evaluation is supported by numerous workers including Taylor (4, 7) and Colby (29) using the index matching fluid, α -toluene.

Changes in incident angle (ϕ) effect both the pathlength through the fiber and the refractive index of the extraordinary ray. The refractive index of the extraordinary ray (n_e) at any incident angle is given by

$$\frac{1}{(n_e)^2} = \frac{\sin^2 \phi}{(n_e^{90})^2} + \frac{\cos^2 \phi}{(n_o)^2},$$

where ϕ is the incident angle (averaged for effect of diffracted beam), n_e^{90} is the refractive index of the extraordinary ray when incident angle equals 90° , and n_o is the refractive index of the ordinary ray. (This ray is always perpendicular to the fiber.)

The depolarization angle attributable to the intrinsic component (δ_i) is then calculated from

$$\delta_i = \frac{360}{\lambda} [d(n_e - n_o)].$$

Since we are interested only in the intrinsic portion of the depolarization, d represents the pathlength through the thick filaments only and not the pathlength through the fiber. (The depolarization caused by the thin

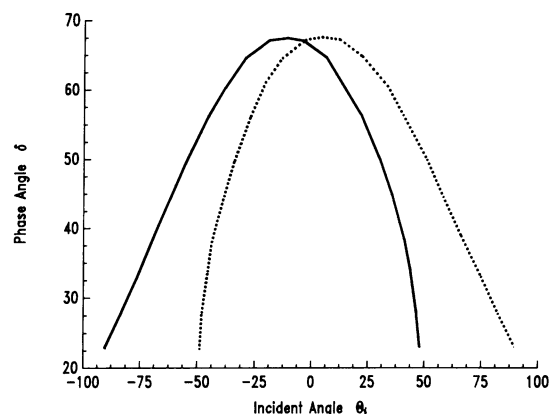


FIGURE 13 Variation in phase angle (δ) with incident angle (θ_i). Left order (solid line); right order (dotted line). 60 μ m diameter fiber; SL = 2.5 μ m. ($\phi = 90^\circ - |\theta_i|$).

filaments is assumed to be small and is not considered in this estimate of δ_i .) The value of d may be calculated from $d = Md_F$, where M is the volume fraction of myosin ($M = 6.8\%$) and d_F is the distance through fiber at given value of ϕ .

Taking a value of $n_o = 1.563$ and $n_e^{90} = 1.576$ the relationship between ϕ and δ_T may be determined. This relationship is shown in Fig. 13 for a 60- μ m diameter fiber at a sarcomere length of 2.5 μ m. From this figure we see that while a $+10^\circ$ change in incident angle has no effect on the right order line, it changes δ_T measured from the left order line by 2–3°.

The authors are grateful for the expert sample preparations carried out by Ms. Quan You.

This work was supported in part by a grant from the National Institutes of Health to Y. Yeh and R. J. Baskin (AM 26817) and by a grant from the National Science Foundation (PCM 83-00046) to R. J. Baskin.

Received for publication 5 July 1985 and in final form 3 February 1986.

REFERENCES

1. Ueno, H., M. E. Rodgers, and W. F. Harrington. 1983. Self-association of a high molecular weight subfragment-2 of myosin induced by divalent metal ions. *J. Mol. Biol.* 168:207–228.
2. Thomas, D. D. J. C. Seidel, J. S. Hyde, and J. Gergely. 1975. Motion of S-1 in myosin and its supramolecular complexes: saturation transfer electron paramagnetic resonance. *Proc. Natl. Acad. Sci. USA.* 72:1729–1733.
3. Yeh, Y., and B. G. Pinsky. 1983. Optical polarization properties of the diffraction spectra from single muscle fibers of skeletal muscle. *Biophys. J.* 42:83–90.
4. Taylor, D. L. 1975. Birefringence changes in vertebrate striated muscle. *J. Supramol. Struct.* 3:181–191.
5. Yeh, Y., M. E. Corcoran, R. J. Baskin, and R. L. Lieber. 1983. Optical depolarization changes on the diffraction pattern in the transition of skinned muscle fibers from relaxed to rigor state. *Biophys. J.* 44:343–351.
6. Barron, L. D. 1982. *Molecular Light Scattering and Optical Activity*. Cambridge University Press, Cambridge. 107–148.
7. Taylor, D. L. 1976. Quantitative studies on the polarization optical properties of striated muscle. *J. Cell Biol.* 68:497–511.
8. Irving, M. 1984. Time-resolved measurements of optical retardation in frog isolated muscle fibres. *J. Physiol. (Lond.)* 353:64.
9. Mendelson, R. A., and P. Cheung. 1976. Muscle crossbridges: absence of direct effect of calcium on movement away from the thick filaments. *Science (Wash. DC)* 194:190–192.
10. Chiao, Y., and W. F. Harrington. 1979. Cross-bridge movement in glycerinated rabbit psoas muscle. *Biochemistry* 18:959–963.
11. Ueno, H., and W. F. Harrington. 1981. Conformational transition in the myosin hinge upon activation of muscle. *Proc. Natl. Acad. Sci. USA.* 78:6101–6105.
12. Reisler, E., and J. Liu. 1982. Conformational changes in the myosin subfragment-2 effect of pH on synthetic rod filaments. *J. Mol. Biol.* 157:659–669.
13. Applegate, D., and E. Reisler. 1983. Crossbridge release and α -helix-coil transition in myosin and rod minifilaments. *J. Mol. Biol.* 169:455–469.
14. Ueno, H., and W. F. Harrington. 1984. An enzyme-probe method to detect structural changes in the myosin rod. *J. Mol. Biol.* 173:35–61.
15. Born, M., and E. Wolf. 1980. *Principles of Optics*. Pergamon Press, New York. Sixth Ed. 705–708.
16. Rome, E. 1968. X-ray diffraction studies of the filament lattice of striated muscle in various bathing media. *J. Mol. Biol.* 37:331–344.
17. Bragg, W. L., and A. B. Pippard. 1953. The form birefringence of macromolecules. *Acta Crystallogr. Sect. B. Struct. Crystallogr. Cryst. Chem.* 6:865–867.
18. Fabiato, A., and F. Fabiato. 1979. Calculator programs for computing the composition of the solutions containing multiple metals and liquids used for experiments in skinned muscle cells. *J. Physiol. (Paris)* 75:463–505.
19. April, E. W., P. W. Brandt, and G. F. Elliott. 1973. The myofibril lattice: studies on isolated fibers. *J. Cell Biol.* 53:53–65.
20. Ueno, H., and W. F. Harrington. 1981. Cross-bridge movement and the conformational state of the myosin hinge in skeletal muscle. *J. Mol. Biol.* 149:619–640.
21. Kawai, M., and P. W. Brandt. 1976. Two rigor states in skinned crayfish single muscle fibers. *J. Gen. Physiol.* 68:267–280.
22. Umazume, Y., and N. Kasuga. 1984. Radial stiffness of frog skinned muscle fibers in relaxed rigor conditions. *Biophys. J.* 45:783–788.
23. Taylor, K. A., M. C. Reedy, L. Cordova, and M. K. Reedy. 1984. Three-dimensional reconstruction of rigor insect flight muscle from tilted thin sections. *Nature (Lond.)* 310:285–291.
24. Rome, E. 1967. Light and x-ray diffraction studies of the filament lattice of glycerol-extracted rabbit psoas muscle. *J. Mol. Biol.* 27:591–602.
25. Matsubara, I., and G. F. Elliott. 1972. X-ray diffraction studies on skinned single fibers of frog skeletal muscle. *J. Mol. Biol.* 72:657–669.
26. Millman, B. M., K. Wakabayashi, and T. J. Racey. 1983. Lateral forces in the filament lattice of vertebrate striated muscle in the rigor state. *Biophys. J.* 41:259–267.
27. Blinks, J. R. 1965. Influence of osmotic strength on cross-section and volume of isolated single muscle fibers. *J. Physiol. (Lond.)* 177:42–57.
28. Rome, E. 1972. Relaxation of glycerinated muscle: low-angle x-ray diffraction studies. *J. Mol. Biol.* 65:331–345.
29. Colby, R. H. 1971. Intrinsic birefringence of glycerinated myofibrils. *J. Cell Biol.* 51:763–771.